Available online at www.sciencedirect.com
ScienceDirect
Tetrahedron
Tetrahedron 63 (2007) 8831–8839

NMR, FTIR, ESI-MS and semiempirical study of a new 2-(2-hydroxyethoxy)ethyl ester of monensin A and its complexes with alkali metal cations

Adam Huczyński, Piotr Przybylski and Bogumil Brzezinski*

Faculty of Chemistry, A. Mickiewicz University, Grunwaldzka 6, 60-780 Poznan, Poland

Received 22 March 2007; revised 22 May 2007; accepted 7 June 2007
Available online 10 June 2007

Abstract—A new 2-(2-hydroxyethoxy)ethyl ester of monensin A (MON6) has been synthesized and its ability to form complexes with Li^+, Na^+ and K^+ cations has been studied by ESI-MS, ^1H and ^{13}C NMR, FTIR, and PM5 semiempirical methods. It is demonstrated that MON6 has been able to form stable complexes of 1:1 stoichiometry with monovalent metal cations. The structures of the complexes are stabilized by intramolecular hydrogen bonds in which the OH groups are always involved. In the structure of MON6 the oxygen atom of the C═O ester group is involved in very weak bifurcated intramolecular hydrogen bonds with two hydroxyl groups whereas in the complexes of MON6 with monovalent metal cations the C═O ester group is not engaged in any intramolecular hydrogen bonds. The structures of the MON6 and its complexes with Li^+, Na^+ and K^+ cations are visualized.

1. Introduction

Monensin A isolated from *Streptomyces cinnamonensis* is a well-known representative of natural polyether ionophore antibiotics. It is able to form pseudomacrocyclic complexes with mono and divalent cations and transport of the cations across cell membranes.[1–5] The pharmacological and biological activity of monensin is based on its ability to disrupt the Na^+/K^+ ion balance across cell membranes, which finally leads to the cell death. Monensin is used commercially as a coccidiostat for poultry and as a growth promoter for ruminants.[6–19]

In our earlier papers the synthesis and the physicochemical characterization of new esters of monensin A has been reported.[20–26] In these publications, the complexation of the mono- and di-valent metal cations by the esters of monensin A and the properties of these complexes have been described in detail. Interestingly one of these esters, namely the methyl ester of monensin A, has been shown to be able to form hydrates with three hydrogen-bonded water molecules inside a pseudo-ring structure. By the self-assembly process this hydrate species forms a proton channel in which the proton can move within the whole channel.[26]

As a continuation of our earlier papers, we report here ESI-MS, ^1H and ^{13}C NMR, FTIR, and PM5 studies of complexes between a new 2-(2-hydroxyethoxy)ethyl ester of monensin A and biologically important monovalent cations such as Li^+, Na^+ and K^+. This new ester, in comparison with the esters studied earlier, contains additionally one etheric and one hydroxylic oxygen atom, which can influence the complexation process. The structure of 2-(2-hydroxyethoxy)ethyl ester of monensin A and its complexes with monovalent cations are discussed in detail.

2. Results and discussion

The molecular structure of MON6 together with the atom numbering is shown in Figure 1. In the present study, we synthesized this ester by the condensation of monensin A with diethylene glycol in the presence of 1,3-dicyclohexylcarbodiimide (DCC) under the addition of 4-pyrrolidinopyridine (PPy) as a very effective acylation catalyst. It is interesting to note that without the addition of PPy the respective ester was not formed.

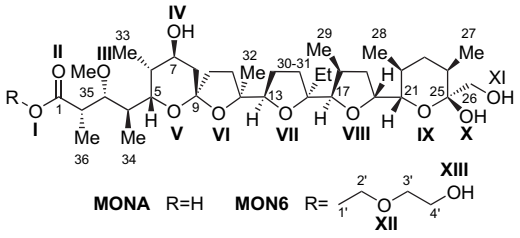

Figure 1. The structures and atom numbering of MONA and MON6.

Keywords: Monensin A; Esters; Complexes; Monovalent cations; Spectroscopy; Hydrogen bonds.
* Corresponding author. E-mail: bbrzez@amu.edu.pl

0040–4020/$ - see front matter © 2007 Elsevier Ltd. All rights reserved.
doi:10.1016/j.tet.2007.06.022

2.1. Electrospray ionization mass spectrometry (ESI) measurements

The main *m/z* signals in the ESI mass spectra of MON6 with the Li^+, Na^+ and K^+ cations used separately at various cone voltages (cv) are summarized in Table 1. According to the data summarized in Table 1, with the cations used in this study MON6 exclusively forms complexes of 1:1 stoichiometry being very stable up to about cv=30 V. Starting from cv=50 V the fragmentation of the respective complexes is observed and it increases with increasing cv values. The proposed fragmentation pathways starting from structure A are shown in Figure 2. The first step of the fragmentation is the loss of one water molecule as a result of the abstraction of the $O_{IV}H$, O_XH or $O_{XIII}H$ hydroxyl groups yielding the B, H or J cation structures, respectively. Further fragmentation of cation B, of MON6 with Li^+ and Na^+ cations, is realized in three directions and other types of complexes [(i) C, E and finally G; (ii) D, F and finally G; or (iii) K] are formed. Cation C is formed from cation B by the abstraction of the second water molecule. The formation of the D and E fragmentary complexes is achieved by abstraction of the part of the molecule including the ester group. Cations F and G can be formed from cations D and E by abstraction of one C_3H_4 group. Additionally, cation G can be formed by loss of one water molecule from cation F. For the complex of MON6 with K^+ cation, no abstraction of the part of the molecule including the ester group was detected.

Table 1. The main peaks in the ESI mass spectra of the complexes of MON6 with cations at various cone voltages

Cation	Cone voltage [V]	Main peaks *m/z*
Li^+	10	766
	30	766
	50	766, 748
	70	766, 748, 734,
	90	766, 748, 734, 269
	110	766, 748, 734, 485,467, 445, 427, 269
	130	485,467, 445, 427, 269
Na^+	10	782
	30	782
	50	782, 764
	70	782, 764, 746
	90	782, 764, 746, 501, 443, 285
	110	782, 764, 746, 507, 501, 483, 461, 443, 285
	130	782, 764, 746, 507, 501, 483, 461, 443, 285
K^+	10	798
	30	798
	50	798, 780, 762
	70	798, 780, 762
	90	798, 780, 762
	110	798, 780, 762
	130	(many peaks)

In the case of the MON6–Na complex the fragmentation of cation B yields cation L, which after the abstraction of one CO molecule forms cation M. Further, cation M undergoes fragmentations typical of other metal cations with

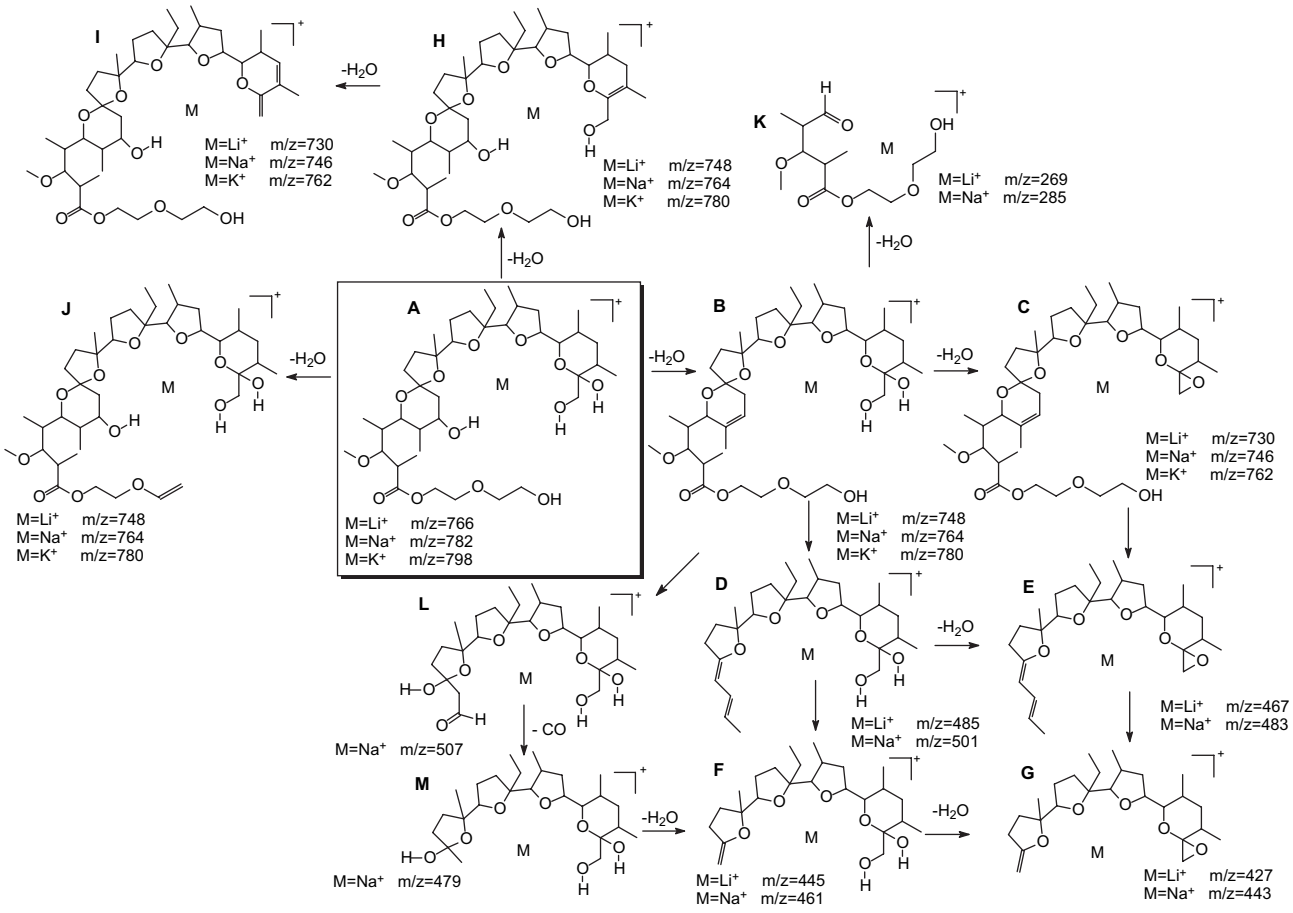

Figure 2. The proposed fragmentation pathways of MON6 complexes with monovalent cations.

abstraction of water molecules in two steps yielding cations F and G, respectively.

The ESI mass spectrum of the 1:1:1:3 mixture of Li^+, Na^+, K^+ cations with MON6 (data not shown), measured at cv=30 V, shows three characteristic signals at *m*/*z*=764 (rel int. 20%), *m*/*z*=782 (rel int. 100%), and *m*/*z*=798 (rel int. 17%), which are assigned to the 1:1 complexes of MON6 with Li^+, Na^+ and K^+ cations, respectively. The intensities of the signals of the MON6–Li^+ and MON6–K^+ complexes are comparable, but significantly lower than that of the MON6–Na^+ complex, demonstrating that MON6 shows much lower affinity to Li^+ and K^+ cations.

2.2. ^{1}H and ^{13}C NMR measurements

The ^{1}H and ^{13}C NMR data of MON6 in CD_3CN and its 1:1 complexes with Li^+, Na^+ and K^+ cations, all in CD_3CN, are summarized in Tables 2 and 3, respectively. Unfortunately, in contrast to the complexes described above, the respective MON6 complexes with $RbClO_4$ and $CsClO_4$ are almost insoluble in acetonitrile. The ^{1}H and ^{13}C signals were assigned independently using one- and two-dimensional (COSY, HETCOR) spectra as well as after the addition of CD_3OD to the probe.

In the ^{1}H NMR spectra of MON6 and its 1:1 complexes with Li^+, Na^+ and K^+ cations (Table 2, Fig. 3) the signals assigned to the protons of the four OH groups are separated. In the spectrum of MON6 the OH proton signals are observed at 2.88, 3.90, 4.15, and 2.93 ppm, and are assigned to $O_{XI}H$, O_XH, $O_{IV}H$, and $O_{XIII}H$ groups, respectively. In the spectra of MON6 complexes with the Li^+, Na^+ and K^+ cations these signals are shifted in different directions depending on the nature of the cation. This spectral feature demonstrates that depending on the cation, the respective hydroxyl groups form different hydrogen bonds related to formation of different structures of the respective complexes. Figure 3 shows that the most significantly shifted signal of the hydroxyl group protons is found in the spectrum of MON6 with Li^+ cation at about 5.76 ppm. This signal is assigned to the $O_{IV}H$ proton, which is involved in the strongest intramolecular hydrogen bond in comparison with those made by all other hydroxyl groups. It is interesting to note that in the spectra of MON6 complexes with Na^+ and K^+ cations, the signals of the $O_{IV}H$ protons are shifted strongly toward lower ppm values demonstrating the weakness of the participation of the $O_{IV}H$ protons in the other types of hydrogen bonds and a probable change of the respective structures of the complexes.

Other proton signals in the ^{1}H NMR spectra of the 1:1 complexes of MON6 with monovalent cations shift only slightly, however, with some exceptions. The most interesting result is the appearance of signals assigned to protons showing double character, which indicates complex conformational changes taking place on the complexation, especially with Li^+ and Na^+ cations.

A comparison of the ^{13}C NMR chemical shifts (Table 3) in the spectra of the complexes studied with those observed in the spectrum of MON6 suggests that not only the oxygen atoms take part in the cations coordination but some more complex conformation changes, evoked by the complexation process, also occur. For instance the $\Delta\delta$ value of the C_{20} atom for the complex of MON6 with Li^+ cation is positive, whereas for the complex of MON6 with Na^+ cation it is negative and for the MON6–K^+ complex it is close to zero. This result indicates that the O_{VIII} oxygen atom is probably involved in the coordination only in the complex of MON6 with Na^+ cation. The ^{13}C NMR signal of the carbonyl C_1 atom of the ester group shifts with the complexation toward higher ppm values, depending on the kind of the cation. This result demonstrates that the intramolecular bifurcated hydrogen bonds between the C_1=O group and the hydroxyl

Table 2. ^{1}H NMR chemical shifts (ppm) of MON6 and its complexes in CD_3CN

No. atom	Chemical shift (ppm)				Differences (Δ) between chemical shifts (ppm)		
	MON6	MON6:Li^+	MON6:Na^+	MON6:K^+	Δ1	Δ2	Δ3
1	—	—	—	—	—	—	—
2	2.63	2.64	2.71	2.67	0.01	0.08	0.04
3	3.58	3.66	3.64	3.52	0.08	0.06	−0.06
4	1.99	2.06	2.04	2.01	0.07	0.05	0.02
5	4.01	4.13	3.92	3.87	0.12	−0.09	−0.14
6	1.78	1.76	1.81	1.78	−0.02	0.03	0.00
7	3.67	3.98	3.91	3.82	0.31	0.24	0.15
8A	1.62	1.54	1.61	1.60	−0.08	−0.01	−0.02
8B	1.97	2.08	2.01	2.00	0.11	0.04	0.03
9	—	—	—	—	—	—	—
10A	1.92	1.84	1.80	1.76	−0.08	−0.12	−0.16
10B	1.92	2.05	2.00	1.89	0.13	0.08	−0.03
11A	1.70	1.57	1.80	1.77	−0.13	0.1	0.07
11B	1.94	2.05	1.99	1.88	0.11	0.05	−0.06
12	—	—	—	—	—	—	—
13	3.65	3.68	3.62	3.51	0.03	−0.03	−0.14
14A	1.58	1.57	1.47	1.43	−0.01	−0.11	−0.15
14B	1.77	1.90	1.90	1.77	0.13	0.13	0
15A	1.56	1.60	1.49	1.44	0.04	−0.07	−0.12
15B	2.09	2.15	2.24	2.20	0.06	0.15	0.11
16	—	—	—	—	—	—	—
17	3.87	4.38	3.96	3.95	0.51	0.09	0.08
18	2.27	2.46	2.30	2.35	0.19	0.03	0.08
19A	1.46	1.58	1.64	1.51	0.12	0.18	0.05
19B	2.15	2.32	2.16	2.22	0.17	0.01	0.07
20	4.19	4.41	4.41	4.37	0.22	0.22	0.18
21	3.61	3.83	3.73	3.64	0.22	0.12	0.03
22	1.32	1.37	1.47	1.31	0.05	0.15	−0.01
23A	1.44	1.32	1.46	1.32	−0.12	0.02	−0.12
23B	1.32	1.41	1.46	1.48	0.09	0.14	0.16
24	1.69	1.88	1.68	1.72	0.19	−0.01	0.03
25	—	—	—	—	—	—	—
26A	3.36	3.45	3.46	3.41	0.09	0.1	0.05
26B	3.36	3.45	3.68	3.62	0.09	0.32	0.26
27	0.84	0.87	0.85	0.84	0.03	0.01	0.00
28	0.86	0.85	0.88	0.86	−0.01	0.02	0.00
29	0.93	0.94	0.89	0.94	0.01	−0.04	0.01
30A	1.57	1.59	1.47	1.50	0.02	−0.1	−0.07
30B	1.57	1.65	1.72	1.70	0.08	0.15	0.13
31	0.89	0.91	0.91	0.92	0.02	0.02	0.03
32	1.35	1.56	1.47	1.46	0.21	0.12	0.11
33	0.90	0.87	0.92	0.89	−0.03	0.02	−0.01
34	0.97	0.98	1.00	0.99	0.01	0.03	0.02
35	3.30	3.33	3.32	3.31	0.03	0.02	0.01
36	1.14	1.18	1.17	1.17	0.04	0.03	0.03
1′	4.21	4.23	4.18	4.21	0.02	−0.03	0.00
2′	3.66	3.70	3.68	3.70	0.04	0.02	0.04
3′	3.52	3.55	3.53	3.54	0.03	0.01	0.02
4′	3.56	3.64	3.63	3.64	0.08	0.07	0.08
$O_{XI}H$	2.88	3.10	4.04	3.26	0.22	1.16	0.38
$O_{IV}H$	4.15	5.76	4.00	3.92	1.61	−0.15	−0.23
O_XH	3.90	4.73	4.45	4.57	0.83	0.55	0.67
$O_{XIII}H$	2.93	4.03	3.03	3.50	1.10	0.10	0.57

$\Delta1=\delta_{MON6:LI^+}-\delta_{MON6}$, $\Delta2=\delta_{MON6:Na^+}-\delta_{MON6}$, $\Delta3=\delta_{MON6:K^+}-\delta_{MON6}$.

Table 3. ^{13}C NMR chemical shifts (ppm) of MON6 and its complexes in CD_3CN

No. atom	Chemical shift (ppm)				Differences (Δ) between chemical shifts (ppm)		
	MON6	MON6:Li^+	MON6:Na^+	MON6:K^+	Δ1	Δ2	Δ3
1	175.75	176.00	177.02	176.39	0.25	1.27	0.64
2	41.42	41.30	41.44	41.74	−0.12	0.02	0.32
3	81.99	81.79	81.76	81.75	−0.20	−0.23	−0.24
4	37.01	37.48	37.95	38.35	0.47	0.94	1.34
5	68.54	69.54	68.95	68.24	1.00	0.41	−0.30
6	36.81	36.42	36.94	36.78	−0.39	0.13	−0.03
7	71.82	70.05	70.74	70.70	−1.77	−1.08	−1.12
8	35.01	33.72	34.57	34.13	−1.29	−0.44	−0.88
9	108.31	108.00	108.32	107.81	−0.31	0.01	−0.50
10	39.68	39.62	39.86	39.97	−0.06	0.18	0.29
11	32.60	33.22	33.42	34.33	0.62	0.82	1.73
12	86.85	87.05	86.60	85.95	0.20	−0.25	−0.90
13	84.32	82.65	82.25	83.44	−1.67	−2.07	−0.88
14	28.40	27.59	27.30	28.30	−0.81	−1.10	−0.10
15	32.02	32.13	30.77	23.08	0.11	−1.25	−8.94
16	87.92	88.00	86.64	86.77	0.08	−1.28	−1.15
17	86.24	84.94	85.46	85.12	−1.30	−0.78	−1.12
18	35.86	34.08	35.03	35.56	−1.78	−0.83	−0.30
19	34.63	33.72	33.79	33.01	−0.91	−0.84	−1.62
20	77.91	79.50	76.93	78.00	1.59	−0.98	0.09
21	77.15	74.71	75.53	75.85	−2.44	−1.62	−1.30
22	33.98	33.30	32.20	32.91	−0.68	−1.78	−1.07
23	37.58	36.96	35.73	36.70	−0.62	−1.85	−0.88
24	37.58	34.69	36.24	35.70	−2.89	−1.34	−1.88
25	97.77	99.51	98.76	98.87	1.74	0.99	1.10
26	67.27	66.55	67.17	67.08	−0.72	−0.10	−0.19
27	16.44	15.99	16.31	17.30	−0.45	−0.13	0.86
28	17.83	17.43	16.64	16.52	−0.40	−1.19	−1.31
29	16.13	16.31	14.47	15.94	0.18	−1.66	−0.19
30	30.05	30.22	30.18	30.50	0.17	0.13	0.45
31	8.29	8.47	8.12	8.54	0.18	−0.17	0.25
32	26.29	28.42	28.27	27.98	2.13	1.98	1.69
33	11.29	10.76	10.92	10.81	−0.53	−0.37	−0.48
34	12.57	13.02	13.20	12.92	0.45	0.63	0.35
35	58.41	58.52	58.77	58.54	0.11	0.36	0.13
36	12.22	11.57	12.23	12.48	−0.65	0.01	0.26
1′	64.45	64.70	64.78	64.71	0.25	0.33	0.26
2′	69.40	69.54	69.52	69.56	0.14	0.12	0.16
3′	73.16	72.93	73.15	73.07	−0.23	−0.01	−0.09
4′	61.74	61.88	61.82	61.58	0.14	0.08	−0.16

$\Delta1 = \delta_{MON6:LI^+} - \delta_{MON6}$, $\Delta2 = \delta_{MON6:Na^+} - \delta_{MON6}$, $\Delta3 = \delta_{MON6:K^+} - \delta_{MON6}$.

groups in the structure of MON6 (Fig. 7) are broken in the structures of the complexes.

2.3. FTIR studies

In Figure 4a the FTIR spectrum of water-free MON6 (solid line) is compared with the corresponding spectra of its 1:1 complexes with Li^+, Na^+ and K^+ cations, all recorded in acetonitrile solution. The bands assigned to the ν(OH) and ν(C═O) vibrations are shown in Figure 4b and c, in an expanded scale, because according to the NMR data, the most significant changes should be observed in these spectral regions. Most characteristic in the FTIR spectrum of water-free MON6 (Fig. 4b, solid line), are the bands assigned to the ν(OH) vibrations of the O_XH, $O_{XI}H$ and $O_{XIII}H$ groups at 3512 cm^{-1}, and of the $O_{IV}H$ group at ca. 3323 cm^{-1} as well as the band assigned to the ν(C═O) vibration at 1732 cm^{-1}. In the spectrum of the MON6–Li^+ complex (Fig. 4b, dashed line) the intensity of the band at 3512 cm^{-1} decreases and a new one at 3379 cm^{-1} arises. This indicates together with the ^1H NMR results (Table 2

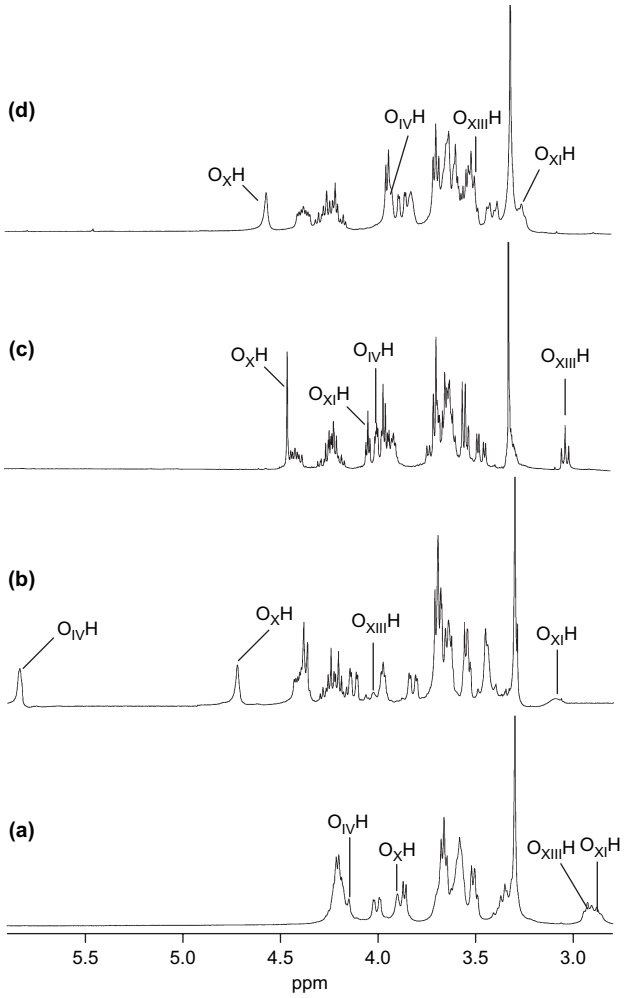

Figure 3. ^1H NMR spectra in the region of the OH proton signals of (a) MON6, (b) MON6–Li^+, (c) MON6–Na^+, and (d) MON6–K^+.

and Fig. 3b) that in the MON6–Li^+ complex the hydrogen bonds of the O_XH and $O_{XIII}H$ groups are slightly stronger than those of $O_{XI}H$ groups and are unchanged if compared to those of uncomplexed MON6. The stretching vibrations of the $O_{IV}H$ group are no longer observed in the spectrum at 3323 cm^{-1}, indicating that the proton of this group is also more strongly hydrogen-bonded.

In the spectrum of the MON5–Na^+ complex (Fig. 4b, dotted line) only one broad band with a maximum at ca. 3479 cm^{-1} was observed demonstrating that the hydrogen bonds formed by the O_XH, $O_{XI}H$ and $O_{XIII}H$ groups become slightly stronger and that of $O_{IV}H$ group slightly weaker. This interpretation is consistent with the ^1H NMR data (Table 2 and Fig. 3c).

Also in the spectrum of MON6–K^+ complex (Fig. 4b, dashed-dotted line) only one band with a maximum at 3501 cm^{-1} is observed indicating that the hydrogen bonds, in which the hydroxyl groups are involved, are weaker compared to the Li^+ and the Na^+ complex and only slightly stronger than in the uncomplexed MON6.

The position of the band assigned to the ν(C═O) vibrations at 1732 cm^{-1}, in the spectrum of MON6 and its complex

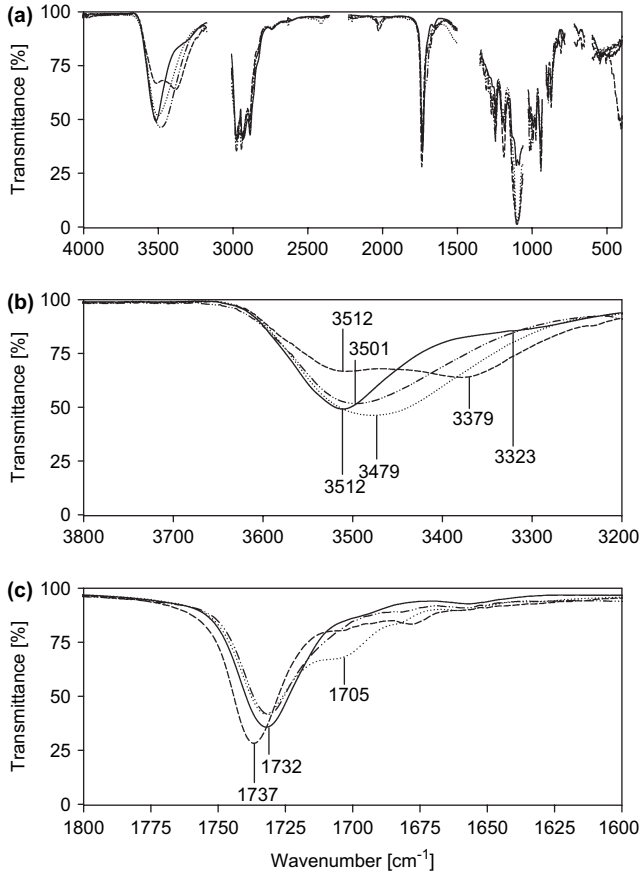

Figure 4. FTIR spectra of (—) MON6, (- - -) MON6–Li^+, (· · ·) MON6–Na^+, and (–· ·–) MON6–K^+ in the range of (a) 4000–400 cm^{-1} and with the expanded scale in the stretching vibrations region, (b) ν(OH), and (c) ν(C═O).

with K^+ cation, is almost unchanged (Fig. 4c), whereas in the case of MON6–Li^+ complex it is slightly shifted toward higher wavenumbers, demonstrating that the oxygen atoms of the C═O ester groups are not engaged in the complexation of these cations. The shift of the band assigned to the ν(C═O) vibrations in the spectrum of MON6–Li^+ complex can be explained by the formation of a hydrogen bond in which the O_I oxygen atom is involved.

The spectrum of the MON6–Na^+ complex is intriguing. Besides the band at ca. 1732 cm^{-1} representing structure A (Fig. 7a), in which the C═O ester group does not contribute to the complexation process, a new less intense band at ca. 1705 cm^{-1} appears. This band can be assigned to the ν(C═O) vibrations in structure B of the MON6–Na^+ complex in which the carbonyl group interacts with the Na^+ cation (Fig. 7b). The low intensity of this new band, however, indicates that structure B is not predominant in acetonitrile solution. The presence of these two bands suggests the existence of a dynamic equilibrium between structure A and structure B of the MON6–Na^+ complex. These two structures are only two extreme conformations among many other conformations realized with different probabilities. For the MON6–Na^+ complex and in contrast to all other complexes investigated here this leads to a gain of entropy. This might explain that Na^+ forms the most stable complexes with MON6 as observed in the ESI experiments discussed above.

2.4. PM5 calculations

Taking into account the experimental findings, the heat of formation (HOF) of the structures of MON6 and its complexes with Li^+, Na^+ and K^+ cations were calculated and are summarized in Table 4. These data show that the most stable complexes in the gas phase (under the experimental conditions similar to those of ESI measurements) are formed with the $Na^+ \gg Li^+ \sim K^+$ cations. This result is in good agreement with the ESI data discussed above. The ΔHOF values show that the structures in which the carbonyl group is involved in the complexation process are energetically less favorable than those in which the carbonyl group is not involved in the complexation process. This is especially significant in the case of MON6–K^+ complexes.

The interatomic distances between the oxygen atoms of MON6 and cations, and the partial charges at these atoms are given in Table 5. Analysis of these values shows that some oxygen atoms such as O_{IV}, O_{VI}, O_{VII}, O_{IX}, and O_{XI} are always involved in coordination irrespective of the kind of the cation, whereas O_I, O_{II},O_{III}, and O_{XII} play no role in this coordination process within the structures of A type, which is in agreement with the ^{13}C NMR data. Other oxygen atoms can be involved in this process depending on the type of cation and the structure A or B. The coordinating distances and the number of coordinating oxygen atoms suggest that all the cations studied can undergo fast fluctuations within the structures of the complexes as it was demonstrated in the complexes of crown ethers with monovalent cations.[27]

Furthermore, the lengths and angles of the hydrogen bonds in which the OH groups are engaged are summarized in Table 6. The calculated structure of MON6 indicates that the O_{II} oxygen atom from the C═O ester group is engaged in the bifurcated intramolecular hydrogen bonds with two O_XH and $O_{XI}H$ hydroxyl groups. On formation of MON6 complexes with cations, these hydrogen bonds are always broken. For this reason, the ^{13}C NMR signals of the C_1 carbon atoms are shifted toward higher ppm values (Table 3).

Table 4. Heat of formation (kcal/mol) of MON6 and its complexes with the cations without (A) and with (B) the engagement of carbonyl group in coordination process calculated by PM5 method (WinMopac 2003)

Complex	HOF (kcal/mol)	ΔHOF (kcal/mol)
MON6	−650.40	—
MON6+$Li^+_{uncomplexed}$(A)	−520.92	−174.77
MON6+$Li^+_{complexed}$(A)	−695.69	
MON6+$Li^+_{uncomplexed}$(B)	−520.92	−111.48
MON6+$Li^+_{complexed}$(B)	−632.40	
MON6+$Na^+_{uncomplexed}$ (A)	−501.28	−254.79
MON6+$Na^+_{complexed}$ (A)	−756.07	
MON6+$Na^+_{uncomplexed}$(B)	−501.28	−219.36
MON6+$Na^+_{complexed}$ (B)	−720.64	
MON6+$K^+_{uncomplexed}$(A)	−492.50	−161.12
MON6+$K^+_{complexed}$(A)	−653.62	
MON6+$K^+_{uncomplexed}$ (B)	−492.50	−79.08
MON6+$K^+_{complexed}$ (B)	−571.58	

$\Delta HOF = HOF_{MON6+M+complexed} - HOF_{MON6+M+uncomplexed}$, where M= monovalent metal cation. (A)—structure of MON6 complex in which the C_1═O group is not involved in coordination of the metal cation. (B)—structure of MON6 complex in which the C_1═O group is involved in coordination of the metal cation.

Table 5. The interatomic distances (Å) and partial charges for O atoms of MON6 coordinating metal cations in complexes structures calculated by PM5 method

Complex with monovalent cation	Monovalent cation partial charge	Coordinating atom	Coordinating atom partial charge	Distances (Å) coordinating atom→cation
MON6: Li^+ (A)	+0.434	O_I	—	—
		O_{II}	—	—
		O_{III}	—	—
		$O_{IV}H$	−0.372	2.00
		O_V	—	—
		O_{VI}	−0.395	2.14
		O_{VII}	−0.377	2.04
		O_{VIII}	—	—
		O_{IX}	−0.384	2.08
		O_X	—	—
		O_{XI}	−0.397	2.16
		O_{XII}	—	—
		O_{XIII}	−0.388	2.09
MON6: Na^+ (A)	+0.297	O_I	—	—
		O_{II}	—	—
		O_{III}	—	—
		$O_{IV}H$	−0.402	2.27
		O_V	—	—
		O_{VI}	−0.408	2.30
		O_{VII}	−0.401	2.26
		O_{VIII}	−0.397	2.21
		O_{IX}	−0.416	2.32
		O_X	—	—
		O_{XI}	−0.400	2.21
		O_{XII}	—	—
		O_{XIII}	—	—
MON6: Na^+ (B)	+0.329	O_I	—	—
		O_{II}	−0.513	2.37
		O_{III}	—	—
		$O_{IV}H$	−0.408	2.29
		O_V	—	—
		O_{VI}	−0.409	2.31
		O_{VII}	−0.513	2.37
		O_{VIII}	−0.402	2.25
		O_{IX}	−0.415	2.32
		O_X	—	—
		O_{XI}	−0.410	2.31
		O_{XII}	—	—
		O_{XIII}	—	—
MON6:K^+ (A)	+0.468	O_I	—	—
		O_{II}	—	—
		O_{III}	—	—
		$O_{IV}H$	−0.420	2.77
		O_V	−0.434	2.81
		O_{VI}	−0.413	2.64
		O_{VII}	−0.438	2.88
		O_{VIII}	—	—
		O_{IX}	−0.435	2.82
		O_X	—	—
		O_{XI}	−0.416	2.72
		O_{XII}	—	—
		O_{XIII}	−0.418	2.75

The strongest hydrogen bonds within the calculated structure of MON6–Li^+ complex are $O_{IV}H\cdots O_{IX}$ and $O_XH\cdots O_{IV}$ intramolecular hydrogen bonds. These results as well as other calculated parameters of the hydrogen bonds are in very good agreement with the NMR and FTIR observations.

The calculated structures of MON6 and its complexes with Li^+, Na^+ and K^+ cations are visualized in Figures 5–8. The hydrogen bonds and the coordination bonds are marked by dots. A comparison of all the calculated structures indicates that only for the MON6 complex with Na^+ cation does the molecule form a pseudo-crown ether structure and therefore, the affinity of MON6 toward Na^+ is higher than that toward other cations.

Table 6. The length (Å) and angle (°) of the hydrogen bond for MON6 complexes calculated by PM5 method (WinMopac 2003)

Compound	O-atom	Hydrogen bond length (Å) [hydrogen bond angle (°)]			
		$O_{IV}H$	O_XH	$O_{XI}H$	$O_{XIII}H$
MON6	O_{II}	—	2.92 [147.4]	2.94 [136.7]	—
	O_{IX}	2.72 [160.9]	—	—	—
	O_{III}	—	—	—	2.96 [143.7]
MON6:Li^+ (A)	O_{IV}	—	2.55 [158.1]	—	—
	O_{III}	—	—	—	—
	O_I	—	—	2.94 [160.8]	2.46 [121.7]
	O_{IX}	2.45 [145.3]	—	—	—
MON6:Na^+ (A)	O_{IV}	—	2.66 [162.7]	—	—
	O_{III}	—	—	2.72 [159.3]	—
	O_X	—	—	—	2.79 [128.2]
MON6:Na^+ (B)	O_{IV}	—	2.65 [148.9]	—	—
	O_{XII}	—	—	2.70 [142.8]	—
	O_X	—	—	—	2.81 [144.8]
MON6:K^+ (A)	O_I	—	2.62 [151.8]	—	—
	O_X	—	—	—	2.78 [147.5]
	O_{III}	—	—	2.75 [139.5]	—

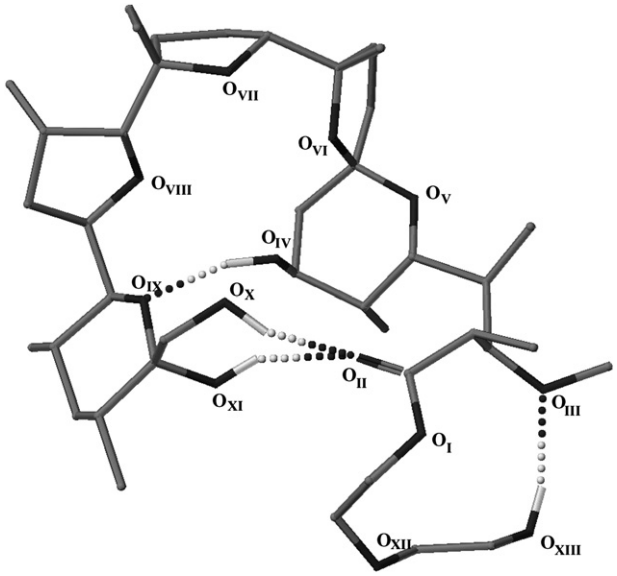

Figure 5. The structure of MON6 calculated by PM5 method (WinMopac 2003).

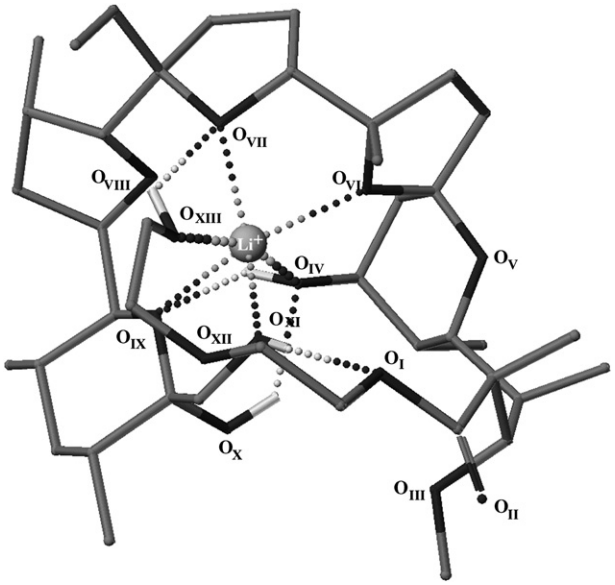

Figure 6. The structure of MON6–Li^+ complex calculated by PM5 method (WinMopac 2003).

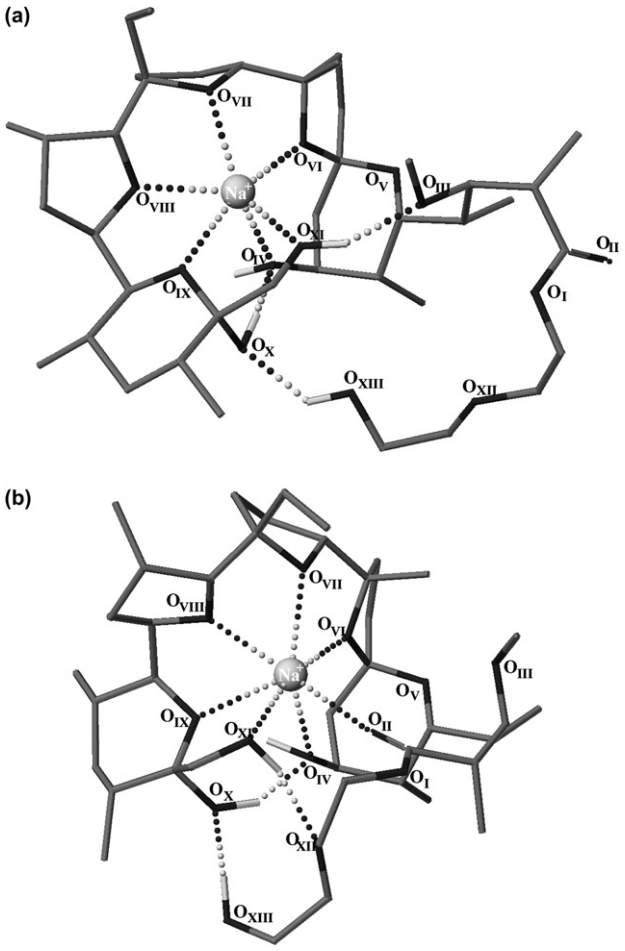

Figure 7. The structures of two types of MON6–Na^+ complexes: (a) without the engagement of the C_1=O carbonyl group in coordination of the cation—type A, (b) with the engagement of the C_1=O carbonyl group in coordination of the cation—type B calculated by PM5 method (WinMopac 2003).

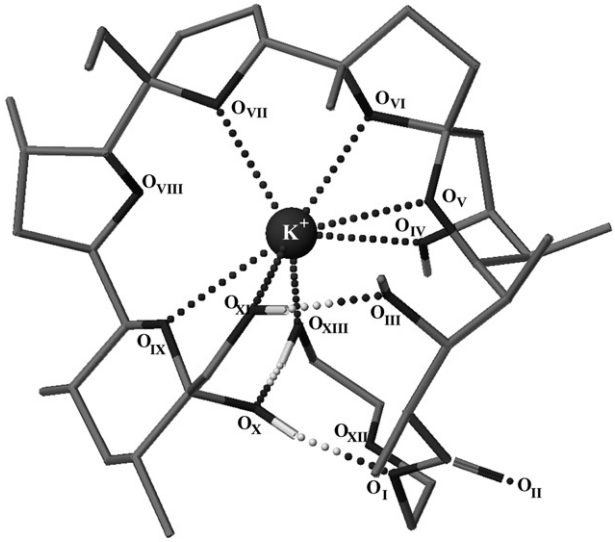

Figure 8. The structure of MON6–K^+ complex calculated by PM5 method (WinMopac 2003).

3. Conclusions

The monensin A ester with diethylene glycol has been synthesized by a new method and its ability to form complexes with Li^+, Na^+ and K^+ cations has been studied. It has been demonstrated that MON6 preferentially forms a complex with Na^+ cations. The formation of stable complexes of 1:1 stoichiometry up to cv=30 V is indicated by the electrospray ionization mass spectra. With increasing cone voltage value the fragmentation of the respective complexes is detected and is connected primarily with the dehydration process. The formation of the complexes as well as the intramolecular hydrogen bonds stabilizing their structures is demonstrated by ^1H and ^{13}C NMR, FTIR spectra and PM5 semiempirical calculations. It is shown that in the structure of MON6 the oxygen atom of the C=O ester group is involved in very weak bifurcated hydrogen bonds with two hydroxyl groups. Within the complexes of MON6 with Na^+ cations (type A), the C=O ester group is not hydrogen-bonded, whereas in the structures of type B it coordinates the Na^+ cations. Such structures are, however, not dominant. It is demonstrated that the strongest intramolecular hydrogen bonds are formed within structure of the MON6–Li^+ complex. Despite this fact, the formation of a pseudo-crown ring structure in the MON6 complex with Na^+ cations determines its highest stability from among all complexes studied.

4. Experimental

4.1. Chemical reagents

The monensin A sodium salt was purchased from Sigma (90–95%). The perchlorates $LiClO_4$, $NaClO_4$ and $KClO_4$ were commercial products of Sigma and were used without any further purification. The salts were hydrates, and it was necessary to dehydrate them by several (6–10 times) evaporation steps from a 1:5 mixture of acetonitrile and absolute ethanol. The dehydration of the perchlorates was followed by FTIR spectroscopy in acetonitrile.

CD_3CN and CH_3CN spectral-grade solvents were stored over 3 Å molecular sieves for several days. All manipulations with the substances were performed in a carefully dried and CO_2-free glove box.

4.2. Synthesis of 2-(2-hydroxyethoxy)ethyl ester of monensin A (MON6)

Monensin A sodium salt was dissolved in dichloromethane and stirred vigorously with a layer of aqueous sulfuric acid (pH=1.5). The organic layer containing MONA was washed with distilled water, and dichloromethane was evaporated under reduced pressure to dryness.

A solution of MONA (500 mg, 0.75 mmol), 1,3-dicyclohexylcarbodiimide (140 mg, 0.90 mmol), 4-pyrrolidinopyridine (50 mg, 0.33 mmol), diethylene glycol (795 mg, 7.5 mmol) in dichloromethane (15 mL) was stirred at a temperature below 0 °C for 24 h. After this time the reaction mixture was stirred at room temperature for 24 h, diluted with H_2O, and extracted with CH_2Cl_2. The extract was evaporated under reduced pressure to dryness. The residue was suspended in hexane and filtered off. The filtrate was evaporated under reduced pressure and purified by chromatography on silica gel (Fluka type 60, dichloromethane/acetone=10:1) to give MON6 (400 mg, 70% yield) as a colorless oil showing tendency to form a glass state. Elementary analysis: Calcd: C, 63.30%; H, 9.30%. Found: C, 63.20%; H, 9.35%.

4.3. Preparation of MON6 complexes with monovalent cations

The solutions (0.07 M) of 1:1 complexes of MON6 with monovalent cations (Li^+, Na^+, and K^+) were obtained by adding an equimolar amount of $MClO_4$ salt (M=Li, Na, K) dissolved in acetonitrile to MON6 dissolved in acetonitrile. The solvent was evaporated under reduced pressure to dryness and the oil residue was dissolved in the respective volume of dry CH_3CN or CD_3CN.

4.4. Mass spectrometry

The ESI (electrospray ionization) mass spectra were recorded on a Waters/Micromass (Manchester, UK) ZQ mass spectrometer equipped with a Harvard Apparatus syringe pump. All samples were prepared in acetonitrile. The measurements were performed with two types of samples; solutions of MON6 (5×10^{-5} mol dm^{-3}) with (a) each of the cations Li^+, Na^+, and K^+ (2.5×10^{-4} mol dm^{-3}) taken separately and (b) the cations Li^+, Na^+, and K^+ (5×10^{-5}/3 mol dm^{-3}) taken together. The samples were infused into the ESI source using a Harvard pump at a flow rate of 20 μL min^{-1}. The ESI source potentials were capillary 3 kV, lens 0.5 kV, extractor 4 V. The standard ESI mass spectra were recorded at cone voltages: 10, 30, 50, 70, 90, 110, and 130 V. The source temperature was 120 °C and the desolvation temperature was 300 °C. Nitrogen was used as the nebulizing and desolvation gas at flow rates of 100 and 300 dm^3 h^{-1}, respectively. Mass spectra were acquired in the positive ion detection mode with unit mass resolution at a step size of 1 *m*/*z* unit. The mass range for ESI experiments was from *m*/*z*=200 to 1000.

4.5. Spectroscopic measurements

The FTIR spectra of MON6 and its 1:1 complexes (0.07 mol dm^{-3}) with $LiClO_4$, $NaClO_4$, and $KClO_4$ were recorded in the mid infrared region in acetonitrile solutions using a Bruker IFS 113v spectrometer.

A cell with Si windows and wedge-shaped layers was used to avoid interferences (mean layer thickness 170 μm). The spectra were taken with an IFS 113v FTIR spectrophotometer (Bruker, Karlsruhe) equipped with a DTGS detector; resolution 2 cm^{-1}. The Happ-Genzel apodization function was used. All manipulations with the compounds were performed in a carefully dried and CO_2-free glove box.

The NMR spectra of MON6 and its 1:1 complexes (0.07 mol dm^{-3}) with $LiClO_4$, $NaClO_4$ and $KClO_4$ were recorded in CD_3CN solutions using a Varian Gemini 300 MHz spectrometer. All spectra were locked to the deuterium resonance of CD_3CN.

The ^{1}H NMR measurements in CD_3CN were carried out at the operating frequency 300.075 MHz; flip angle, pw=45°; spectral width, sw=4500 Hz; acquisition time, at=2.0 s; relaxation delay, d_1=1.0 s; T=293.0 K and using TMS as the internal standard. No window function or zero filling was used. Digital resolution was 0.2 Hz per point. The error of chemical shift value was 0.01 ppm.

^{13}C NMR spectra were recorded at the operating frequency 75.454 MHz; pw=60°; sw=19,000 Hz; at=1.8 s; d_1=1.0 s; T=293.0 K and TMS as the internal standard. Line broadening parameters were 0.5 or 1 Hz. The error of chemical shift value was 0.01 ppm.

The ^{1}H and ^{13}C NMR signals were assigned independently for each species using one or two-dimensional (COSY, HETCOR) spectra.

4.6. PM5 calculations

PM5 quantum calculations were performed using the WinMopac 2003 program at the semiempirical level (Cache Work System Pro Version 5.04—Fujitsu).[28–32] PM5 quantum semiempirical method uses the Schrödinger equation to determine bond strengths, atomic hybridizations, partial charges, and orbitals from the positions of the atoms and the net charge.

For MON6 and its complexes the initial optimization of the structures was carried out using the molecular mechanics—extensive global minimum energy conformation search with the Conflex/MM3 from WinMopac 2003 program. Global optimization runs were carried out for all the MON6 complexes using about 4500 local minimizations in each global optimization. The calculated energetically the most favorable structures of conformers corresponding the global minimum points were further optimized by the PM5 quantum semiempirical method with the energy gradient not exceeding 10 kcal mol^{-1} in one step. In all cases full geometry optimization of MON6 and its complexes was carried out without any symmetry constraints. The semiempirical calculations were performed using a computer equipped with an

AMD Athlon 1.26 GHz processor and 2GB operating memory.

4.7. Elemental analysis

The elemental analysis of MON6 was carried out on Vario ELIII (Elementar, Germany).

Acknowledgements

A.H. wishes to thank the Foundation for Polish Science for fellowship. Financial assistance of the Polish Ministry of Science and Higher Education–Grant No. N204 056 32/1432 is gratefully acknowledged by P.P. The authors thank the Polish Ministry of Science and Higher Education for financial support under Grant No. R 0501601.

References and notes

1. Riddell, F. G. *Chirality* **2002**, *14*, 121–125.
2. Martinek, T.; Riddell, F. G.; Wilson, C.; Weller, C. T. *J. Chem. Soc., Perkin Trans. 2* **2000**, 35–42.
3. Ferdani, R.; Gokel, G. W. *Encyclopedia of Supramolecular Chemistry: Ionophores*; Marcel Dekker: New York, NY, 2004; pp 760–766.
4. Westley, J. W. *Polyether Antibiotics. Naturally Occurring Acid Ionophores*; Marcel Dekker: New York, NY, 1982; Vol. 1, pp 1–20.
5. Westley, J. W. *Polyether Antibiotics. Naturally Occurring Acid Ionophores*; Marcel Dekker: New York, NY, 1983; Vol. 2, pp 51–86.
6. Pressman, B. C. *Antibiotics and their Complexes*; Marcel Dekker: New York, NY, 1985; pp 1–18.
7. Edrington, T. S.; Callaway, T. R.; Varey, P. D.; Jung, Y. S.; Bischoff, K. M.; Elder, R.; Anderson, R. C.; Kutter, E.; Brabban, A. D.; Nisbet, D. J. *J. Appl. Microbiol.* **2003**, *94*, 207–213.
8. Stephen, B.; Rommel, M.; Daugschies, A. *Vet. Parasitol.* **1997**, *69*, 19–29.
9. McGuffey, R. K.; Richardson, L. F.; Wilkinson, J. I. D. *J. Dairy Sci.* **2001**, *84E*, 194–203.
10. Haimoud, D. A.; Bayourthe, C.; Moncoulon, R.; Verney, M. *J. Sci. Food Agric.* **1996**, *70*, 181–191.
11. Ipharraguerre, I. R.; Clark, J. H. *Anim. Feed Sci. Technol.* **2003**, *106*, 39–57.
12. Ramanzin, M.; Bailoni, L.; Schiavon, S.; Bittante, G. *J. Dairy Sci.* **1997**, *80*, 1136–1142.
13. Richardson, L. F.; Raun, A. P.; Potter, E. L.; Cooley, C. O. *J. Anim. Sci.* **1974**, *39*, 250–256.
14. Tanabe, K. *Blood Cells* **1990**, *16*, 437–449.
15. Adovelande, J.; Schrevel, J. *Life Science* **1996**, *59*, 309–315.
16. Bergstrom, R. C.; Maki, L. R. *J. Am. Vet. Med. Assoc.* **1978**, *165*, 288–295.
17. Donoho, A. L. *J. Anim. Sci.* **1984**, *58*, 1528–1539.
18. Mollenhauer, H. H.; Morre, D. J.; Rowes, R. D. *Biochim. Biophys. Acta* **1990**, *1031*, 225–246.
19. Iacoangeli, A.; Melucci-Vigo, G.; Risuleo, G. *Biochimie* **2000**, *82*, 35.
20. Huczyński, A.; Przybylski, P.; Brzezinski, B.; Bartl, F. *Biopolymers* **2006**, *81*, 282–294.
21. Huczyński, A.; Przybylski, P.; Brzezinski, B.; Bartl, F. *Biopolymers* **2006**, *82*, 491–503.
22. Huczyński, A.; Michalak, D.; Przybylski, P.; Brzezinski, B.; Bartl, F. *J. Mol. Struct.* **2006**, *797*, 99–110.
23. Huczyński, A.; Michalak, D.; Przybylski, P.; Brzezinski, B.; Bartl, F. *J. Mol. Struct.* **2007**, *828*, 130–141.
24. Huczyński, A.; Przybylski, P.; Brzezinski. *J. Mol. Struct.* **2006**, *788*, 176–183.
25. Huczyński, A.; Przybylski, P.; Schroeder, G.; Brzezinski, B. *J. Mol. Struct.* **2007**, *29*, 111–119.
26. Huczyński, A.; Przybylski, P.; Brzezinski, B.; Bartl, F. *J. Phys. Chem. B* **2006**, *110*, 15615–15623.
27. Brzezinski, B.; Schroeder, G.; Rabold, A.; Zundel, G. *J. Phys. Chem.* **1995**, *99*, 8519–8523.
28. Stewart, J. J. P. *Method J. Comp. Chem.* **1989**, *10*, 209–220.
29. Stewart, J. J. P. *Method J. Comp. Chem.* **1991**, *12*, 320–341.
30. CAChe 5.04 UserGuide, Fujitsu 2003.
31. Przybylski, P.; Huczyński, A.; Brzezinski, B. *J. Mol. Struct.* **2007**, *826*, 156–164.
32. Huczyński, A.; Ratajczak-Sitarz, M.; Katrusiak, A.; Brzezinski, B. *J. Mol. Struct.* **2007**, *832*, 84–89.